3-D visual data compression based on ray-space projection

Takeshi Naemura, Masahide Kaneko and Hiroshi Harashima

Department of Information and Communication Engineering,
The University of Tokyo, 7-3-1 Hongo, Bunkyo-ku, Tokyo 113, Japan
e-mail : naemura@hc.t.u-tokyo.ac.jp
URL: http://www.hc.t.u-tokyo.ac.jp/index-e.html

ABSTRACT

As 2-D image communication systems come into use widely, 3-D imaging technology enhancing the reality of visual communication is getting to be considered as a promising next-generation medium that can revolutionize information systems. To date, 3-D image communication has not been discussed at a comprehensive level because several kinds of promising 3-D display technologies are still making rapid progress. Considering such a situation, this paper introduces the concept of the “Integrated 3-D Visual Communication System”. The key feature in this new concept is a display-independent neutral representation of visual data. The flexibility of this concept will promote the progress of 3-D image communication systems before the 3-D display technology reaches maturity. In this paper, for this purpose, ray-based approach is examined. In the present representation method, the whole ray data is equally treated as a set of orthogonal views of the scene objects. The advantage of this approach is to allow the synthesis of any perspective view by gathering appropriate ray data from the set of orthogonal views independently of any geometric representation. A real-time progressive transmission method has been also examined. The experimental results show how the present representation method could be applied to the next-generation 3-D image communication system.

keywords : 3-D image coding, 3-D image processing, virtual reality, display-independent representation of visual data, Ray-Space, ray-based representation, direction-uniform projection, orthogonal views, progressive coding, image-based rendering

1 INTRODUCTION

As 2-D image communication systems come into use widely, 3-D imaging technology enhancing the reality of visual communication by providing natural depth sensation is getting to be considered as a promising next-generation medium that can revolutionize information systems. The construction of 3-D image communication systems will require the development of various constituent technologies : 3-D image capture, 3-D description, 3-D transmission, 3-D display, 3-D handling and so on. To date, 3-D image communication has not been discussed at a comprehensive level because several kinds of promising 3-D display technologies (such as binocular glasses, head mount displays (HMDs), lenticular methods, parallax barrier methods, focused-beam arrays, holographic methods and eye-position tracking methods) are still making rapid progress. From this point of view, most of the works on 3-D image processing can be seen as specialized methods for limited combination of input and output technologies : stereopairs,[1] multi-view[2] images and holography.[3]

Considering such a situation, the authors proposed the concept of the “Integrated 3-D Visual Communication Systems”[4] illustrated in Figure 1. The key feature in this new concept is a display-independent representation of visual data; all the differences of representation between the input and the output methods will be absorbed by the neutrality of the representation for any format of visual data. So it allows us to select our favorite way of observing the transmitted 3-D images regardless of the input method. The flexibility of this concept will promote the progress of 3-D image communication systems before the 3-D display technology reaches maturity.

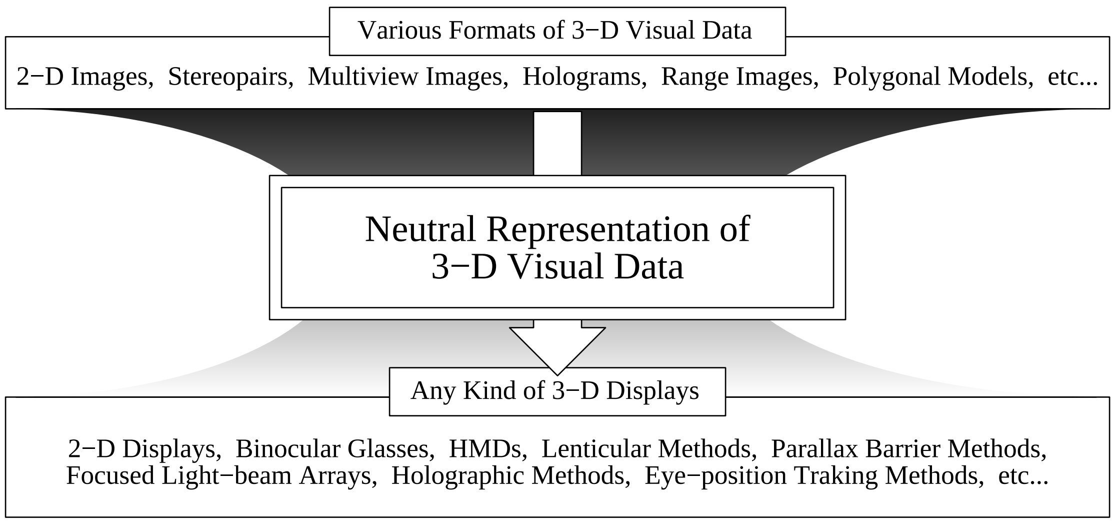

Figure 1: Basic concept of the “Integrated 3-D Visual Communication System”[4].

The authors have been investigating and comparing two practical methods for the neutral representation of 3-D visual data : (a) structure-based approach and (b) ray-based approach.

It is straightforward that the structure-based representation is practical way of displaying scene objects. In such a context, the various techniques in computer graphics will play an important role because they have already provided an appropriate way of representing structures. Structural properties, however, are not necessarily convenient for some formats of the input data. To solve this problem, a great deal of improvement in the field of structure recovery will be required.

In this paper, the ray-based approach, first developed by Fujii[5] for the purpose of a neutral representation, is examined. Its key feature is that only the true visual data is transmitted, the recognition of structural properties being left to the observer. This results in the reduction of the necessity of structure recovery from the input data. Recently, a similar concept, called image-based rendering, was applied in the field of computer graphics to avoid the difficulties in synthesizing polygonal models of the real world.[6–9] In these applications, rays are parameterized by the position of their intersection with cylindrical and plane surfaces. This leads, however, to inaccuracy for directions of rays that are parallel to the surfaces. This paper deals with a new 3-D representation method in which the whole visual data is equally treated as a set of orthogonal views of the objects and the surroundings. The advantage of this approach is to allow the synthesis of any perspective view by gathering appropriate ray data from the set of orthogonal views independently of any geometric representation. A progressive transmission method has been also examined.

2 RAY-BASED REPRESENTATION OF VISUAL DATA

Since the visual sensation is excited by rays of light incident on the retina, each of these rays can be seen as a primitive element of visual data. So, any format of visual data can be decomposed into a set of such ray data. Conversely, arbitrary visual data suitable for the displaying technology can be synthesized by gathering appropriate ray data. A ray can be identified by the coordinates (X, Y, Z) of passing point in the space and the set (θ, ϕ) representing its azimuth and elevation angle of propagation. Therefore, by providing a five-dimensional parametric space (X, Y, Z, θ, ϕ), ray data at any point in any direction (should it be power or wavelength) can be stored separately. This parametric space is called the "Ray-Space"[5,10,11] or "Plenoptic Function"[7–9,12] and is represented in the form of $f(X, Y, Z, \theta, \phi)$. In this paper, these concepts are developed to a 3-D representation method in which the whole visual data is equally treated as a set of orthogonal views of the objects and the surroundings.

Using this function, 2-D image data, captured from a viewpoint (X_a, Y_a, Z_a) using a pinhole camera, can be represented as follows (Figure 2(a)) : $f(\theta, \phi)|_{X=X_a, Y=Y_a, Z=Z_a}$. This means that a 2-D image corresponds to a 2-D sub-space of a 5-D Ray-Space.[5] In the same way, as illustrated in Figure 2(b), it can be said that a hologram plane $Z = g(X, Y)$ contains ray data within the 4-D sub-space $f(X, Y, \theta, \phi)|_{Z=g(X,Y)}$. Thus, any kind of visual data can be mapped onto the 5-D Ray-Space. Conversely, by sampling the appropriate ray data from the 5-D Ray-Space, arbitrary visual data can be synthesized.

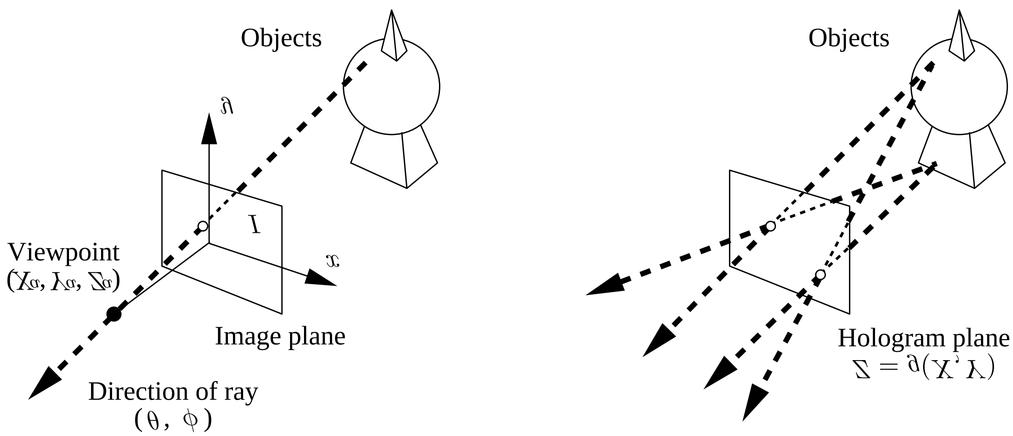

(a) Rays recorded on an image.

(b) Rays recorded on a hologram.

Figure 2: Rays seen as primitive elements of visual data.

Since the epipolar plane image,[13] synthesized from a set of 2-D images, can be also embedded in this 5-D Ray-Space, the present concept is also useful for the purpose of structure recovery. However, the goal of our flexible 3-D image communication system is the transmission of this 5-D Ray-Space [†]. Since the present work aims to allow the full transmission of the whole Ray-Space, it should erase the necessity of a computer-based recognition of the included structures left here to the observer.

3 FORMULATION OF RAY-SPACE PROJECTION

3.1 From a 5-D Ray-Space to a 4-D subspace

The 5-D Ray-Space contains the whole ray data. Using this ray-based representation, any visual application of a given 3-D space (such as view synthesis at arbitrary viewpoints and stereoscopic visual effects) can be performed. However, this representation requires tremendous amount of apparently redundant data. Considering its application to transmission,

[†] The word "3-D image" may mean that the observers can select their viewpoints in the 3-D space. As mentioned before, the representation of 3-D images, however, requires a 5-D data space. To avoid this confusing situation, we may be encouraged to use the word "space communication" instead of "3-D image communication".

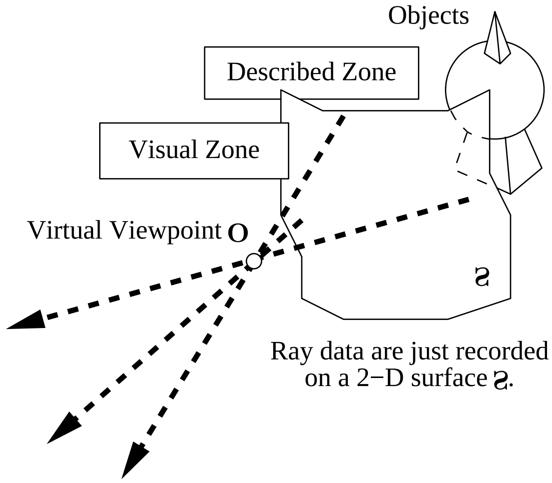

Figure 3: By gathering ray data on a surface **S**, a virtual view at a viewpoint **O** can be synthesized.

an effective data compression method of the Ray-Space, aimed to save the whole previously described necessary data, is strongly required.

In this paper, we consider the case where ray data is just recorded on a surface **S** (See Figure 3). 3-D space is divided by **S** into two zones; visual zone and described zone. If the position of any point on **S** can be represented by two parameters P and Q, the whole ray data can be mapped onto a 4-D Ray-Space $f(P, Q, \theta, \phi)$. Thus, the set of rays intersecting the surface **S** is stored in a reduced 4-D Ray-Space. By assuming that rays go straight on without any variation in the direction of propagation, we can even synthesize a virtual view at a viewpoint **O**. By constructing several views within the inside of visual zone, we can easily provide the autostereoscopic visual effects.

Figure 4 illustrates two types of applications of the surface **S**. If the rays, going out of the bounded region, are recorded, we can observe the objects placed within this region from any direction with a natural depth feeling. Conversely, if rays, concentrating into this region, are recorded, we can enjoy this stereoscopic effect all around us. Thus, this method is useful for several kinds of visual applications, such as multiplex hologram and CAVEs. The conclusion is that, in many cases, a 4-D Ray-Space is enough to describe 3-D images and allows an efficient description of 3-D images.

3.2 Projection of the Ray-Space

It is required for the sake of neutrality, that the projection from a 5-D Ray-Space onto a 4-D one should be independent of the shape of surface **S**. In this section, such a “direction-uniform” projection[10] (method previously developed by the authors) is explained.

For simplicity, we illustrates the discussion with the 3-D Ray-Space $f(X, Z, \theta)$ shown in Figure 5. In the first step, ray vectors of the Figure 5(a) are mapped onto the Ray-Space $f(X, Z, \theta)$ illustrated in Figure 5(b). The related Figure 5(c), illustrating the same Ray-Space $f(X, Z, \theta)$, shows how a ray-axis R parallel to the ray direction is defined for each θ. Another axis P is also defined for each θ. By twisting the Ray-Space $f(X, Z, \theta)$ around θ-axis, all the ray-axes R are aligned in the same direction (See Figure 5(d)), leading to convert $f(X, Z, \theta)$ into the Ray-Space $f(P, R, \theta)$. This process can also be seen as a simple coordinate transformation. In the 3-D Ray-Space $f(P, R, \theta)$, ray variation (such as attenuation or interference in the direction of propagation) is recorded along the ray-axis R. By assuming that rays go straight on without any variation along the direction of propagation, an $f(P, R, \theta)$ space can be projected onto an $f(P, \theta)$ plane. Thus, the 3-D Ray-Space $f(X, Z, \theta)$ has been projected onto a 2-D one without losing any data of the individual rays.

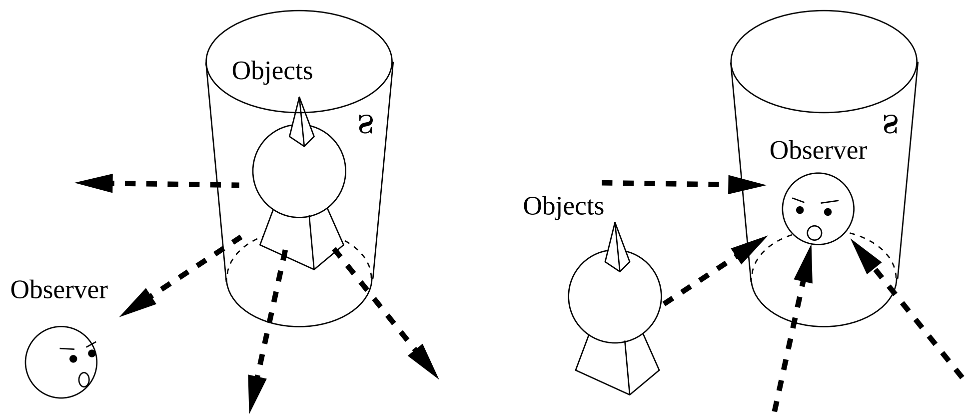

(a) 3-D object representation

(b) 3-D surroundings representation

Figure 4: Applications of the surface $\mathbf{S}$; (a) When rays going out of the bounded region are recorded, we can observe the objects placed within the region from any direction with a natural depth sensation. (b) By recording the rays concentrating into this region, we can enjoy the same stereoscopic effect all around us.

3.3 Formulation of Projection

In this section, the above Ray-Space projection is formulated. Before projecting the Ray-Space in the direction of propagation of the rays, the coordinate system (X, Y, Z) is transformed into that one (P, Q, R) where R represents the ray direction. Considering that the 3-D vectors $\mathbf{p}$, $\mathbf{q}$ and $\mathbf{r}$ are linearly independent, any arbitrary vector $[X, Y, Z]^T$ can be represented by the linear combination

$$[X, Y, Z]^T = P\,\mathbf{p} + Q\,\mathbf{q} + R\,\mathbf{r}. \tag{1}$$

Figure 6 illustrates some examples of PQR coordinate systems with various definition of 3-D vectors $\mathbf{p}$, $\mathbf{q}$ and $\mathbf{r}$. In all the examples, ray-axis $\mathbf{r}$ is defined as follows :

$$\mathbf{r} = [\,\sin\theta\cos\phi,\ \sin\phi,\ \cos\theta\cos\phi\,]^T. \tag{2}$$

Some possible variation in the projection methods are provided by the redefinition of the other axes P and Q.

3.3.1 Planer coordinate system

A simple example illustrated in Figure 6(a) is to define two 3-D vectors $\mathbf{p}$ and $\mathbf{q}$ as follows :

$$\mathbf{p} = [\,1,\ 0,\ 0\,]^T, \quad \mathbf{q} = [\,0,\ 1,\ 0\,]^T. \tag{3}$$

In this case, one PQ-plane is just provided for all directions of rays. Ignoring the R coordinate, the following equations can be derived from the Equations (1), (2) and (3).

$$P = X - Z\tan\theta, \quad Q = Y - Z\frac{\tan\phi}{\cos\theta} \tag{4}$$

Using these equations, the 5-D function $f(X, Y, Z, \theta, \phi)$ is converted into a 4-D function $f(P, Q, \theta, \phi)$. The merit of this type of projection is that the calculation cost is lower than that of other projection methods. This method, however, cannot equally treat all the directions of rays; it can not store, for example, such rays that do not intersect with the defined PQ-plane (i.e. that are parallel to X or Y axis).

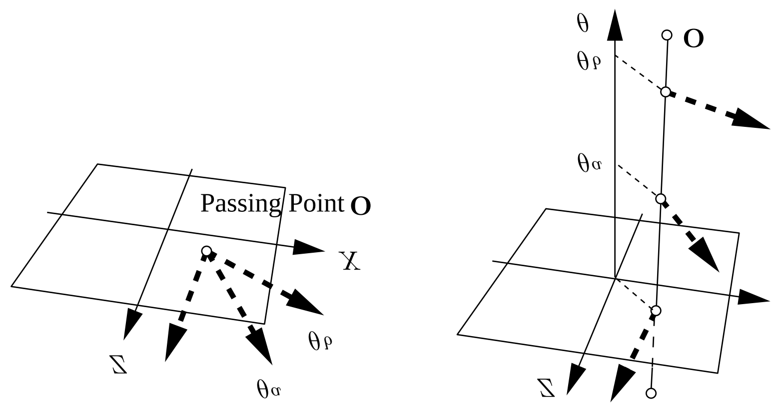

(a) Ray vectors in the real world. (b) 3-D Ray-Space $f(X, Z, \theta)$

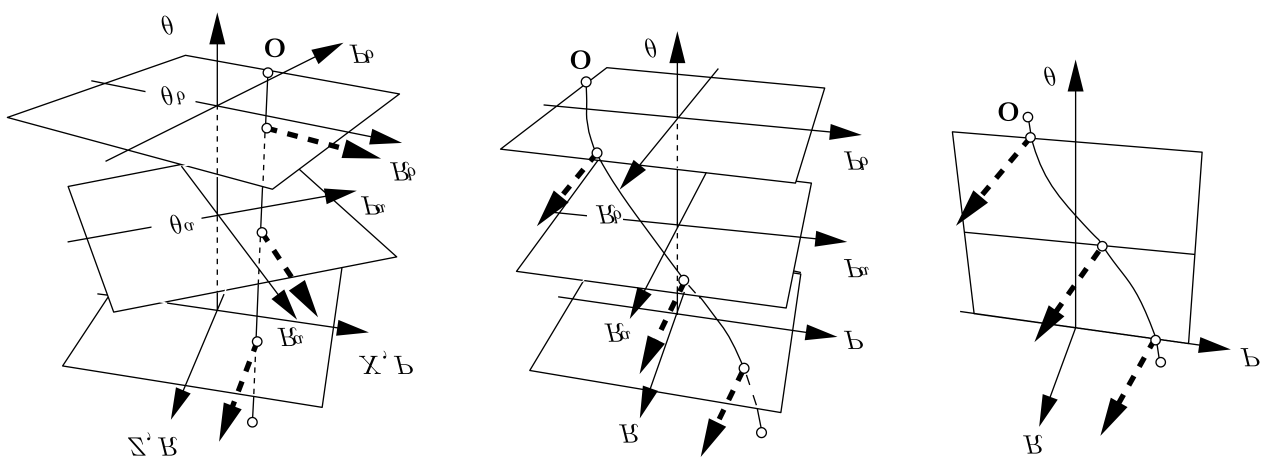

(c) Definition of ray-axis R (d) $f(P, R, \theta)$ as twisted (c) (e) 2-D Ray-Space $f(P, \theta)$

Figure 5: 3-D Ray-Space $f(X, Z, \theta)$ example of Ray-Space projection[10].

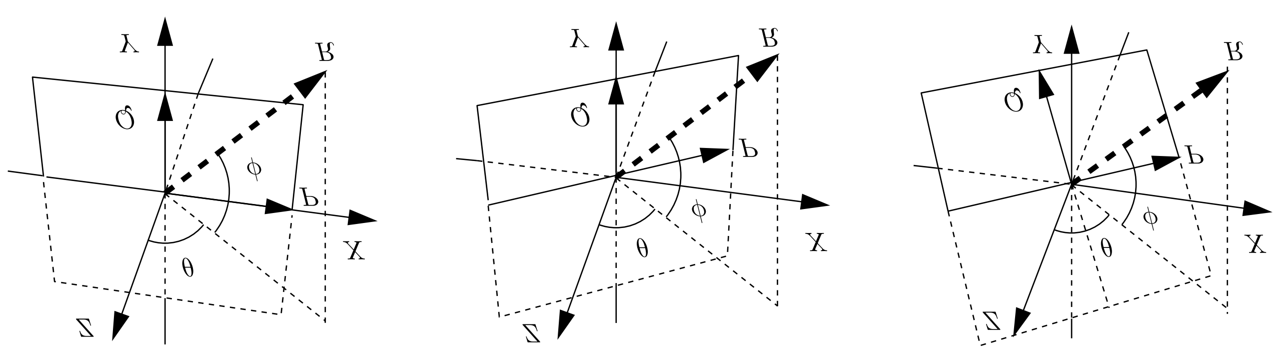

(a) Planer coordinate system (b) Cylindrical coordinate system (c) Spherical coordinate system

Figure 6: Examples of PQR coordinate systems[10].

3.3.2 Cylindrical coordinate system

In the same way, if we assume $\mathbf{p}$ and $\mathbf{q}$ to be such as :

$$\mathbf{p} = [\,\cos\theta,\ 0,\ -\sin\theta\,]^T, \quad \mathbf{q} = [\,0,\ 1,\ 0\,]^T, \tag{5}$$

the following equations are derived for Figure 6(b).

$$P = X\cos\theta - Z\sin\theta, \quad Q = -X\sin\theta\tan\phi + Y - Z\cos\theta\tan\phi. \tag{6}$$

Using these equations, a 5-D $f(X, Y, Z, \theta, \phi)$ is converted into a 4-D $f(P, Q, \theta, \phi)$. As a PQ-plane is provided for each θ, this method can store rays parallel to X axis. It is, however, still unable to cope with rays parallel to Y axis.

3.3.3 Spherical coordinate system

Finally, if $\mathbf{p}$ and $\mathbf{q}$ are as follows † :

$$\mathbf{p} = [\,\cos\theta,\ 0,\ -\sin\theta\,]^T, \quad \mathbf{q} = [\,-\sin\theta\sin\phi,\ \cos\phi,\ -\cos\theta\sin\phi\,]^T, \tag{7}$$

the equations bellow are derived for Figure 6(c).

$$P = X\cos\theta - Z\sin\theta, \quad Q = -X\sin\theta\sin\phi + Y\cos\phi - Z\cos\theta\sin\phi. \tag{8}$$

In this case, a ray-axis R parallel to the ray direction and a PQ-plane normal to the R-axis are defined for each direction of rays (θ, ϕ). Therefore, the whole visual data is equally treated by this method. Using these equations, the 5-D $f(X, Y, Z, \theta, \phi)$ is converted into a 4-D $f(P, Q, \theta, \phi)$ without losing any data of the individual rays.

Since $\mathbf{p}$, $\mathbf{q}$ and $\mathbf{r}$ are orthogonal, the PQ-plane defined for each direction of rays (θ, ϕ) is an orthogonal view of the 3-D objects or surroundings. Thus, $f(P, Q, \theta, \phi)$ can be thought as a set of orthogonal views PQ for each ray direction (θ, ϕ). This is the key feature of this method. Hence, even though 3-D image representations based on a collection of perspective views heavily depends on the viewpoint locations of the input data, our method is viewpoint-independent thanks to the use of a collection of orthogonal views. The following discussions will concentrate on this type of 4-D Ray-Space.

4 4-D RAY-SPACE SYSTEM

Based on the equations deduced in the previous section, a 4-D Ray-Space system can be constructed. Framework of this system is illustrated in Figure 7. There are four steps; (a) capture or synthesis of the ray data, (b) analysis or interpolation of the Ray-Space, (c) compression and transmission of the Ray-Space and (d) display or handling of the ray data.

In step (a), any kind of visual input is decomposed into ray data. As this process requires the information of camera position and orientation, the estimation techniques of camera parameters are essential. In this paper, a computer-controlled camera gantry is used to avoid this problem. Figure 8 illustrates the special case in which the image plane is parallel to the XY plane. From this figure, the following equations ‡ can be derived.

$$x = -F\tan\theta, \quad y = -F\frac{\tan\phi}{\cos\theta} \tag{9}$$

† 3-D vectors $\mathbf{p}$, $\mathbf{q}$ and $\mathbf{r}$ are calculated by rotating X,Y,Z-axes around Y and X-axis, respectively.

‡ From the Equations (4) and (9), the following simple equations can be derived : $P = X + Zx/f$, $Q = Y + Zy/f$. Such simplicity provides some merit to the planer coordinate system; low calculation cost, simple structure for analysis and so on.

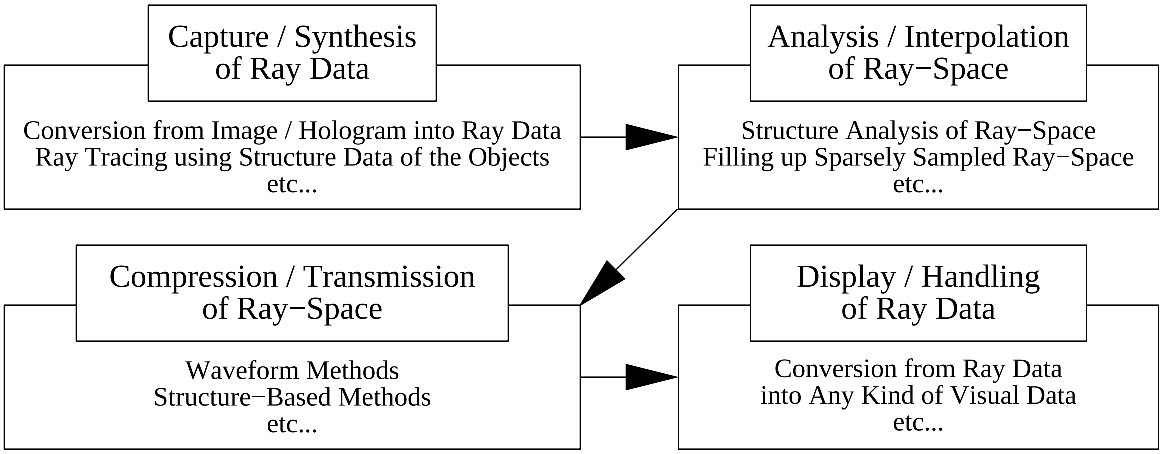

Figure 7: Framework of the ray-based representation of 3-D visual data.

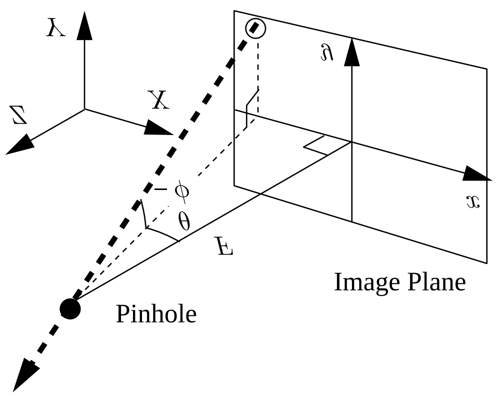

Figure 8: Relationship between the image coordinate (x, y) and the ray direction (θ, ϕ).

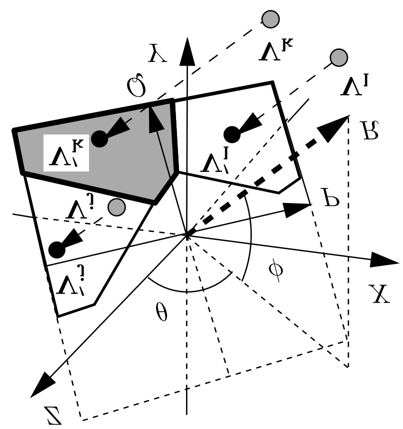

Figure 9: A PQ-plane is divided into some regions, each of which is filled up with synthesized orthogonal view.

where (x, y) denotes the image coordinate, and F focal length. These equations allow us to convert the direction (θ, ϕ) of a ray into its recorded position (x, y). Even if the image plane is not parallel to XY plane, image data can be decomposed into ray data by considering the relationship between the ray direction (θ, ϕ) and the image coordinate (x, y). In the case of a virtual world, ray data will be synthesized by ray tracing techniques.

In many cases, the number of the ray data samples directly provided by the input data is not enough. As a consequence, sparsely sampled Ray-Space is constructed. In order to construct dense Ray-Space, interpolation of the ray data is performed in step (b). For this purpose, segmentation or structure recovery of the Ray-Space can be examined. Since a 4-D Ray-Space is a set of orthogonal views, it is created by the conversion from input perspective views into orthogonal views. In this paper, the following algorithm is applied to fill up each PQ-plane corresponding to a given direction of rays (See Figure 9).

1. A PQ-plane is divided into some regions using Voronoi diagrams whose center points are the shadows of viewpoints. In Figure 9, the viewpoint locations of input data and the shadows of them are denoted by $\mathbf{V_j}, \mathbf{V_k}, \mathbf{V_l}, \cdots$, and $\mathbf{V'_j}, \mathbf{V'_k}, \mathbf{V'_l}, \cdots$, respectively.

2. For each region of the PQ-plane, an orthogonal view is synthesized from the corresponding input view. The conversion from the input perspective view into the orthogonal view exploits the results of disparity estimation between input views; local structure models are prepared for each input view.

3. Cracks on the PQ-planes are filled by median filters.

Since many structural models, resulting from disparity estimations at each view, are adaptively stitched to interpolate ray data, this approach can avoid the difficulties in estimating a unique structure model of the real world. Furthermore, even if the disparity estimation failed, the 4-D Ray-Space is filled up using the median filters.

Since the Ray-Space, even though its dimension is effectively reduced to four, still contains a tremendous amount of data, an efficient compression method is strongly required at the transmission step (c). Waveform, structure-based as well as fractal-based[14] methods, can be examined. In this paper, a progressive method is experimentally demonstrated for the transmission of a 4-D Ray-Space in section 5.

Finally, in step (d), the transmitted Ray-Space is converted into the appropriate format for a 3-D display. When the location of observer (X, Y, Z) is given, the positions of the corresponding ray data in the 4-D Ray-Space are calculated from Equation (8). Then, the sampled ray data is converted into an appropriate view. Some kinds of optical effects can also be added. Furthermore, some Ray-Spaces can be merged to realize virtual worlds.

5 EXPERIMENTAL RESULTS

For the experiment, the multi-view image database, presented by University of Tsukuba is used as the input visual data. This image set consists of 81 views of a toy Santa Claus, parts of them are illustrated in Figure 10. Their camera parameters are given by University of Tsukuba. First of all, for each direction of rays, a corresponding PQ-plane is synthesized by the previously described method. Figure 11 shows some of the results. The resolution of each PQ-plane is 182×182 and the number of such PQ-planes is equal to the resolution of the $\theta\phi$-plane; 300×220. The details of experimental configurations such as the resolution and the quantization steps of each axis are listed in Table 1, which also contains the details of other experimental configurations described later. Thanks to the adaptive use of the input views, we can see that visually natural views are synthesized.

Figure 10: Parts of original multi-view images

Figure 11: Examples of synthesized PQ-planes as orthogonal projections of the object.

Table 1: Experimental configurations

	Complete 4-D Ray-Space	Quantizing P and Q axes	Quantizing θ and ϕ axes
Range of P axis	$-70.2mm < P < 70.2mm$		
Range of Q axis	$-70.2mm < Q < 70.2mm$		
Quantization step size of P and Q axes	$0.77mm$	$6.1mm$	$0.77mm$
No. of sample points of $P \times Q$	182×182	23×23	182×182
Range of θ axis	$-13.0° < \theta < 13.0°$		
Range of ϕ axis	$-9.6° < \phi < 9.6°$		
Quantization step size of θ, ϕ axes	$0.0866°$	$0.0866°$	$0.684°$
No. of sample points of $\theta \times \phi$	300×220	300×220	38×28
Total no. of sample points	2.2×10^9	3.5×10^7	3.5×10^7
Total amount of data $(3bytes/sample)$	6.6 GB	105 MB	105 MB

Figure 12 illustrates the effect of the ray interpolation based on disparity estimation. If ray data is interpolated by assuming a unique disparity for each pixel on the original views, discontinuity between stitched views will appear on a synthesized virtual view (See Figure 12(a)). To solve this problem, the proposed ray interpolation method on each PQ-plane is applied. The virtual view in Figure 12(b) is synthesized from the PQ-planes shown in Figure 11. It can be said that the ray interpolation, based on the disparity estimation, succeeded in avoiding this discontinuity artifact.

(a) Without disparity estimation. (b) Utilizing estimated disparity.

Figure 12: Comparison of the effect of the ray interpolation method.

Figure 13(a) shows various views synthesized from the dense Ray-Space whose amount of data is about 6.6 GB. Thanks to the proposed ray interpolation technique, visually natural views are synthesized. The amount of the dense Ray-Space data, however, is too large to transmit. If the viewpoint location of the observer is measured at the output side, exploiting this information, just the corresponding 2-D subspace of the 4-D Ray-Space can be sent to the observer. This approach, however, is not neutral for any kind of the output method; the whole Ray-Space should be transmitted for the purpose of the neutrality of the system. Thus, the effect of progressive transmission of the whole 4-D Ray-Space is experimentally demonstrated here. The details of experimental configurations are listed in Table 1. If the whole Ray-Space is progressively transmitted, we can see the views synthesized from the already transmitted incomplete Ray-Space during the transmission. If the PQ-planes are progressively transmitted, we will observe such views shown in Figure 13(b). It can be said that the toy Santa Claus is more blurred than the background; the closer the object is, the more the views are blurred. This may be the effect of perspective projection; the closer the object is, the more the views are enlarged. If the $\theta\phi$-planes are progressively transmitted, we will observe such views shown in Figure 13(c). It can be said that the blocking artifacts are more visible in the region of the background than that of the object. This is because the ill effect of the quantization of ray direction grows according to the distance of propagation; the farther the object is, the worse the effect of quantizing ray direction is.

(a) Synthesized from the dense Ray-Space whose amount of data is about 6.6 GB.

(b) Synthesized from the subsampled Ray-Space whose amount of data is about 105 MB. Bandwidth of both P and Q axes are eight times lower than that of (a).

(c) Synthesized from the subsampled Ray-Space whose amount of data is about 105 MB. Resolution of both θ and ϕ axes are eight times lower than that of (a).

Figure 13: Effects of progressive transmission of the Ray-Space. (a) Virtual views synthesized from a completely transmitted Ray-Space. (b) While PQ-planes are being progressively transmitted, virtual views synthesized from an incomplete Ray-Space will be blurred. (c) While $\theta\phi$-planes are being progressively transmitted, blocking artifacts will appear on virtual views.

Considering these features, the authors will develop the progressive method of the whole Ray-Space transmission.

6 CONCLUSIONS

In this paper, the concept of the “Integrated 3-D Visual Communication System” and the “Ray-Space” is introduced, and an efficient data compression method based on Ray-Space projection is proposed. The method how the 5-D Ray-Space is projected on a space of fewer dimension is illustrated and formulated. By using this method, the Ray-Space can be treated systematically. For the purpose of a real-time transmission of the whole Ray-Space, progressive methods are also examined. In the experiments, the resolution of PQ-planes and that of $\theta\phi$-planes are selectively changed. The experimental results show the possibility of the real-time transmission of the whole Ray-Space. The authors will continue to investigate the more effective data compression method for the reduced 4-D Ray-Space and develop various kinds of applications of the ray-based representation : virtual reality, computer graphics, computer vision and so on. Our method is useful and powerful for flexible 3-D image communication systems because of its neutrality and scalability.

7 REFERENCES

[1] M.G.Perkins, “Data compression of stereopairs,” *IEEE Trans. Commun.*, vol. 40, pp. 684 – 696, Apr. 1992.

[2] M.E.Lukacs, “Predictive coding of multi-view point image sets,” in *Proc. IEEE ICASSP’86*, pp. 521 – 524, 1986.

[3] H.Yoshikawa, “Digital holographic signal processing,” in *Proc. First International Symposium on Three Dimensional Image Communication Technologies*, S4-2, TAO, Dec. 1993.

[4] H.Harashima, T.Fujii, and T.Naemura, “Towards integrated 3-D visual communication systems,” Technical Report HC92-58, IEICE, Jan. 1993. (in Japanese).

[5] T.Fujii, *A Basic Study on the Integrated 3-D Visual Communication*. PhD thesis, Dept. of Elec. Eng., The Univ. of Tokyo, Mar. 1995. (in Japanese).

[6] A.Katayama, K.Tanaka, T.Oshino, and H.Tamura, “A viewpoint independent stereoscopic display using interpolating of multi-viewpoint images,” in *Stereoscopic displays and virtual reality system II 2409*, pp. 11 – 20, SPIE, Feb. 1995.

[7] L.McMillan and G.Bishop, “Plenoptic modeling : An image-based rendering system,” in *Proc. SIGGRAPH’95*, pp. 39 – 46, ACM, Aug. 1995.

[8] M.Levoy and P.Hanrahan, “Light field rendering,” in *Proc. SIGGRAPH’96*, pp. 31 – 42, ACM, Aug. 1996.

[9] S.Gortler, R.Grzeszczuk, R.Szeliski, and M.Cohen, “The lumigraph,” in *Proc. SIGGRAPH’96*, pp. 43 – 54, ACM, Aug. 1996.

[10] T.Naemura, T.Yanagisawa, M.Kaneko, and H.Harashima, “Efficient projection of ray space for a ray based description of 3-D real world,” Technical Report IE95-119, IEICE, Feb. 1996. (in Japanese).

[11] T.Fujii, T.Kimoto, and M.Tanimoto, “Ray space coding for 3D visual communication,” in *Proc. PCS’96*, pp. 447 – 451, Mar. 1996.

[12] E.Adelson and J.Bergen, “The plenoptic function and the elements of early vision,” in *Computer Models of Visual Processing* (M.Landy and J.Movshon, eds.), ch. 1, MIT Press, 1991.

[13] H.H.Baker and R.C.Bolles, “Generalizing epipolar-plane image analysis on the spatiotemporal surface,” *Int. Journ. of Computer Vision*, vol. 3, pp. 33 – 49, 1989.

[14] T.Naemura and H.Harashima, “Fractal coding of a multi-view 3-D image,” in *Proc. IEEE ICIP’94*, vol. III, pp. 107 – 111, Nov. 1994.